STEM CELLS AND DEVELOPMENT
Volume 31, Numbers 5–6, 2022

DOI: 10.1089/scd.2021.0302

MED12 Regulates Human Adipose-Derived Stem Cell Adipogenesis and Mediator Kinase Subunit Expression in Murine Adipose Depots

Sree Venigalla,[1] Joseph Straub,[1] Onyekachi Idigo,[1] Caroline Rinderle,[1] Jacqueline M. Stephens,[2] and Jamie J. Newman[1]

The mediator kinase module plays a critical role in the regulation of transcription during metabolic processes. Here we demonstrate that in human adipose-derived stem cells (hASCs), kinase module subunits have distinct mRNA and protein expression profiles during different stages of adipogenesis. In addition, siRNA-mediated loss of MED12 results in decreased adipogenesis as evident through decreased lipid accumulation and decreased expression of PPARγ, a master regulator of adipogenesis. Moreover, the decrease in adipogenesis and reduced PPARγ expression are observed only during the early stages of MED12 knockdown. At later stages, knockdown of MED12 did not have any significant effects on adipogenesis or PPARγ expression. We also observed that MED12 was present in a protein complex with PPARγ and C/EBPα during all stages of adipogenesis in hASCs. In 3T3-L1 preadipocytes and adipocytes, MED12 is present in protein complexes with PPARγ1, C/EBPα, and STAT5A. CDK8, another member of the kinase module, was only found to interact with C/EBPα. We found that the expression of all kinase module subunits decreased in inguinal, gonadal, and retroperitoneal white adipose tissue (WAT) depots in the fed state after an overnight fast, whereas the expression of kinase module subunits remained consistent in mesenteric WAT (mWAT) and brown adipose tissue. These data demonstrate that the kinase module undergoes physiologic regulation during fasting and feeding in specific mouse adipose tissue depots, and that MED12 likely plays a specific role in initiating and maintaining adipogenesis.

Keywords: hASCs, kinase module, mediator complex, MED12, adipogenesis

Introduction

Obesity is a global epidemic that results in insulin resistance, type 2 diabetes mellitus (T2DM), cardiovascular diseases (CVD), metabolic disorders, and certain types of cancers. Obesity is characterized by excess body fat accumulation in adipose tissue that affects the overall health of an individual [1–3]. To better understand how obesity contributes to metabolic disorders and identify potential therapeutic targets, further investigation is needed to elucidate the mechanistic processes that regulate adipogenesis.

In mammals, adipose tissue exists in two main types: brown and white. Brown adipose tissue (BAT) specializes in heat production by exerting its thermogenic function mainly in newborns [4,5]. White adipose tissue (WAT) is most abundant and is responsible for lipid storage distributed as subcutaneous and visceral WAT depots. WAT is linked to metabolic disorders including T2DM and CVD [6–9].

Aberrant adipogenesis is characterized by impaired secretion of various adipokines and results in insulin resistance and an increased risk for T2DM [10,11]. Adipogenesis is the process by which preadipocytes differentiate into mature adipocytes. Adipogenesis is regulated by an elaborate network of transcription factors, of which PPARγ and C/EBPα are considered master regulators [12–17].

Mediator is a large evolutionarily conserved multiprotein complex that functions as a bridge between RNA polymerase II and cell type-specific transcription factors. The

[1]School of Biological Sciences, Louisiana Tech University, Ruston, Louisiana, USA.
[2]Pennington Biomedical Research Center, Baton Rouge, Louisiana, USA.

mediator complex is grouped into four modules: head, middle, tail, and kinase. The mediator kinase module is composed of four subunits, three of which have mutually exclusive paralogs: MED12/L, MED13/L, CDK8/19, and Cyclin C (CCNC) [18–21].

Of these, MED12 stands out as a unique subunit. MED12 has been associated with many cancers, including uterine leiomyomas, fibroadenomas, chronic lymphocytic leukemia, and malignant phyllodes tumors, where mutations in MED12 appear to be most associated with the role of MED12 in activating the kinase activity of CDK8/19 [20,21–23]. MED12 has been found to associate with superenhancers, interact with NANOG, SOX2, and PRC1 in pluripotent stem cells, interact with Wnt/β-Catenin, maintain HSC viability, and interact with SOX10 in glial cells [24–28]. These studies suggest that MED12 is an indispensable component in the regulation of stem cell state.

The kinase module is also involved in metabolism and adipogenesis. The CDK8/CCNC dimer negatively regulates de novo lipogenesis by promoting nuclear SREBP1c protein degradation in mouse liver [29]. In addition, using glycerol gradient fractionation it was shown that the kinase module undergoes dissociation and degradation upon nutrient signaling in mouse livers [30]. However, it remains unclear whether the kinase module subunits are dissociated and degraded in adipose tissue.

In this study, we demonstrate the differential expression of kinase module subunits during adipogenesis of human adipose-derived stem cells (hASCs) and observed that MED12 expression contributes to adipogenesis through PPARγ expression. We also observed the reduced expression of kinase module subunits with refeeding in several mouse adipose tissue depots. This discovery of fluctuations in expression and novel interactions between MED12 and adipogenic transcription factors advances our understanding of the role of MED12 during adipogenesis and introduces mechanisms of crosstalk between transcription regulation and differentiation, creating the possibility for identifying novel therapeutic targets against obesity and its related diseases.

Materials and Methods

In vitro studies using hASCs

Cell culture. hASCs (cell lines 71101, 70926, and 412 purchased from Obatala, Inc.) were cultured in complete culture medium containing αMEM 1× (Cat No. 12561049; Life Technologies), 16.5% fetal bovine serum (Cat No. S11550; Atlanta Biologicals), 1% L-glutamine 200 mM (100×) (Cat No. 25030-081; Gibco), and 1% penicillin streptomycin (Cat No. 15140122; Life Technologies). Cells were incubated at 37°C at 5% CO_2 and medium was changed every 48 h.

siRNA transfection. hASCs were cultured to 30%–50% confluency and transfected with negative control (Cat No. 4390843; Thermo Scientific) and MED12-specific siRNA (5 nmol/mL) (Cat No. s19364; Thermo Fisher Scientific) using Lipofectamine RNAiMAX reagent (Cat No. 13778075; Life Technologies) following manufacturer's protocol.

Inducing adipogenesis. Adipogenesis was induced in cells once they reached 80% confluency through the addition of AdipoQual (LaCell LLC LaADM-500) medium. Medium was changed every 72 h.

Oil Red O staining. Oil Red O stock solution was prepared using 0.5 g of solid Oil Red O (Cat No. 11411–412; VWR) and 100 mL of 100% isopropanol. Working solution was prepared using three parts of Oil Red O stock solution per two parts of distilled water, filtered through a 0.22 μm syringe filter (Cat No. 229747; CELLTREAT). Cells were fixed using a 10% formalin solution and incubated at room temperature for 15 min. Oil Red O was added to fixed cells and incubated for 20 min at room temperature. The cells were imaged using a Cytation 5 BioTek Plate Reader.

RNA extraction and cDNA synthesis. RNA was collected using TRIzol reagent (Cat No. 15596018; Ambion). RNA was extracted following the manufacturer's protocol and quantified using a Take3 plate on a Cytation 5 BioTek Plate Reader. qScript cDNA Supermix (Cat No. 95048-100; VWR) was used to synthesize cDNA using 1 μg of RNA following manufacturer's protocol.

Quantitative reverse transcriptase-PCR. Quantitative reverse transcriptase PCR (qRT-PCR) was performed in technical triplicates using PowerUp SYBR Green Master Mix (CatNo. A25742; Thermo Fisher Scientific), primers, and 1 μL of cDNA. The reaction was run using a StepOnePlus Applied Biosystems machine standard quantitation experiment. The data were plotted in Excel using $\Delta\Delta$ C_T. The primer sequences used are listed in Table 1.

Protein extraction and quantification. Cells were collected using RIPA buffer (Cat No. ab156034; Abcam) with phosphatase and protease inhibitors (Cat No. 88666; Thermo). The cells were agitated for 30 min at 4°C and centrifuged at 4°C (14,000 *g* for 20 min). Protein samples were quantified using Bradford assay (Cat No. 5000006; Bio-Rad).

Western blot. Sodium dodecyl sulfate-polyacrylamide gel electrophoresis (SDS-PAGE) was performed using a Mini

Table 1. List of Primer Sequences Used for qRT-PCR

Gene	*Forward sequence (5′–3′)*	*Reverse sequence (3′–5′)*	*Size (bp)*
gapdh	CCCCACTTGATTTTGGAGGGA	AGGGCTGCTTTTAACTCTGGT	206
med12	CGAAAAGGGACAGCAGAAAC	CCCATCCTCCCCACCTAAGA	87
med13	TGTCCTGCTCCTTCACCTTTT	GGCATAAGATAACTTGAAATGGGCT	150
ccnc	GCTGATTTGATCGAGGAGCG	ATCCATTGCAAATAGTGGGAGC	148
cdk8	GCCAAGAGGAAAGATGGGAAGG	GCCGACATAGAGATCCCAGTT	77
pparγ	GCTGTTATGGGTGAAACTCTG	ATAAGGTGGAGATGCAGGTTC	151
c/ebpα	TATAGGCTGGGCTTCCCCTT	AGCTTTCTGGTGTGACTCGG	94
tubulin1-α	CCAGGGCTTCTTGGTTTTCC	CGCTCAATGTCGAGGTTTCT	167
srebp1c	CTCTTGAAGCCTTCCTGAG	GCACTGACTCTTCCTTGAT	138

qRT-PCR, quantitative reverse transcriptase-PCR.

PROTEAN TGX™. Samples (50–100 μg) were loaded in an SDS-PAGE gel (Cat No. 4561084; Bio-Rad). Proteins were transferred using transblot Turbo™ PVDF transfer pack (Cat No. 88518; Thermo scientific). Membranes were blocked in 5% milk for 2 h in 1 × TBS with 0.1% Tween, probed overnight at 4°C with target primary antibody (Table 2), washed five times, and probed with secondary antibody (1:10,000). The blots were developed and visualized with enhanced chemiluminescent substrate (ECL) and chemiluminescence (Cat No. 1705060; Bio-Rad).

Co-IP assay. Protein was collected as already described but by using IP lysis buffer. The collected protein was agitated for 5 min at 4°C and centrifuged at 13,000 *g* for 10 min. The supernatant was collected and quantified using Bradford assay. Coimmunoprecipitations (Co-IPs) were performed using the Pierce Crosslink Magnetic IP/Co-IP kit following the manufacturer's protocol (Cat No. 88805; Thermo Fisher Scientific). Five microliters of polyclonal antibody was used per 200 μg of lysate. Collected elution and unbound lysates were used for western blot.

Statistical analysis

Data are presented as the mean ± standard error of the mean. Graphs were generated using Student's *t*-test with $P < 0.05$ considered statistically significant.

Mouse studies

All regulations of the institutional animal care and use committee at Pennington Biomedical Research Center were strictly followed. All animal procedures were approved by the Institutional Animal Care and Use Committee at Pennington Biomedical Research Center under protocol number 977, which was approved on October 31, 2016.

Animals. Fourteen-week-old female mice (strain: C57BL6/J) were used for fasting and feeding experiments. Mice were provided 5015 mouse chow. For fasting and feeding experiments, the mice in the fasting group ($n = 3$) were fasted overnight for 14 h and sacrificed the next morning, whereas mice in the fed group ($n = 3$) were provided with food 4 h after 14 h of overnight fasting and were sacrificed after feeding.

Protein extraction and immunoblotting. Fresh mouse fat depot tissues were cut and frozen immediately in liquid nitrogen. The tissues were homogenized in IP buffer for 5–10 s and immediately placed on ice. After centrifugation at 20,000 *g* for 20 min at 4°C, the resulting supernatants were quantified using bicinchoninic acid assay (Cat No. BCA1; Sigma-Aldrich). Equal amounts of protein samples (50 μg) were separated on 5% and 12% SDS gels (acrylamide Cat No. EC-890; National Diagnostics) and transferred to nitrocellulose membrane (Cat No. 162-0115). Antibodies used are listed in Table 2.

Immunoprecipitation assay. 3T3-L1 mouse preadipocytes (originally obtained from Howard Green laboratory at Harvard Medical School) were cultured using cell culture medium (DMEM-Cat No. D5030; Sigma-Aldrich with 10% bovine calf serum Cat No. 16030074; Thermo Scientific). Cells were induced to differentiate using a standard MDI induction cocktail of 0.5 mM 3-isobutyl-1-methylxanthine (MIX), 1 μM dexamethasone, and 1.7 μM insulin in DMEM containing 10% fetal bovine serum (Cat No. A31605; Thermoscientific).

Cell cultures were collected at stages of preadipocytes and mature adipocytes by adding IP buffer, and a mixture of protease and phosphatase inhibitors was added to the collected protein samples. After centrifugation at 13,000 *g* for 10 min at 4°C, the resulting supernatants were quantified using BCA analysis and 200 μg of protein was used for immunoprecipitation. Twenty-five microliters of bead slurry (Protein A/G Plus-Agarose, Cat No. sc-2003; Santa Cruz Biotechnology) was added to protein and rocked for 1 h in the cold room and was spun at 12,000 rpm for 1 min.

Five micrograms of the appropriate polyclonal antibody was added to each sample and incubated on the rocker in the cold room for 1 h or overnight. After the incubation, samples were centrifuged for 1–3 min at 16,000 *g*. Beads were then washed with 1 mL of cold IP buffer and centrifuged for 1–3 min at 11,000 *g*. A sample of whole cell lysate and an IP buffer with no cell lysate were used as negative control to ensure that there was no unspecific binding.

Results

Expression of mediator kinase module subunits fluctuates during adipogenesis

To investigate the potential role of the mediator kinase module in adipogenesis, we examined the gene and protein expression profiles for each of the four subunits in hASCs induced to undergo adipogenesis. Cells were stained using Oil Red O (Fig. 1A) and differentiation was further confirmed through expression of adipogenic markers C/EBPα, PPARγ, and SREBP1C (Fig. 1B, D). We monitored the transcript levels of the kinase module subunits MED12, MED13, CDK8, and CCNC throughout differentiation and noticed varying levels of each subunit at different times during adipogenesis (Fig. 1C).

The expression of *med12* and *ccnc* followed the same trend where expression increased from days 0 to 14 and dropped

Table 2. List of Antibodies Used for Western Blot Analysis

Antibody	*Size (k Da)*	*Host species*	*Company*	*Catalog No.*	*Dilution*
MED12	248	Rabbit	Bethyl Laboratories	A300–774A	1:1,000
MED13	268	Rabbit	Bethyl Laboratories	A301–278A	1:1,000
CDK8	58	Rabbit	Bethyl Laboratories	A302–501A-M	1:1,000
CCNC	28	Rabbit	Bethyl Laboratories	A301–989A	1:1,000
PPARγ	53, 57	Rabbit	ThermoFisher/Santa Cruz Biotechnology	PA3-821A/SC7273	1:500/1:100
C/EBPα	30 and 42	Rabbit	ThermoFisher/Abcam	PA1-337/Ab15048	1:1,000
GAPDH	37	Rabbit	Abcam	Ab9485	1:3,000
α-Tubulin	58	Rabbit	Cell Signaling	2144S	1:2,000
STAT5A	92	Rabbit	Abcam	Ab32043	1:1,000

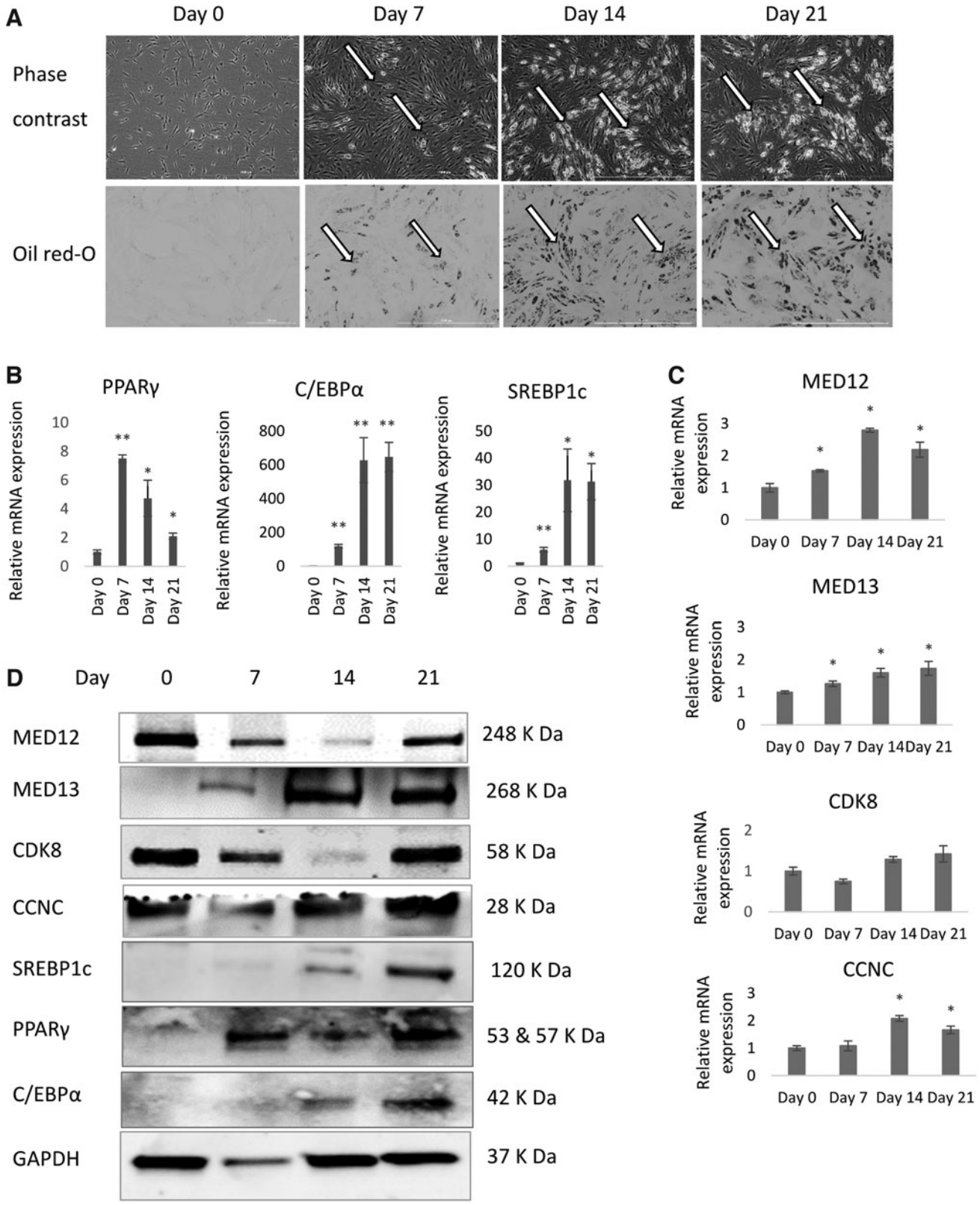

FIG. 1. Expression levels of kinase module subunits fluctuate during hASC adipogenesis. Cultured hASCs were differentiated into adipocytes and collected at different time points ($n=3$). **(A)** Phase contrast microscopy and Oil Red O staining color images of adipogenic differentiation of hASCs at days 0, 3, 7, 14, and 21. Stained lipid droplets are shown with *arrows*. **(B, C)** qRT-PCR of adipogenic genes (*pparγ*, *c/ebpα*, and *srebp1c*) and kinase module subunits (*med12*, *med13*, *cdk8*, and *ccnc*) at days 0, 7, 14, and 21 of adipogenesis**.** *P* values were determined by Student's *t*-test ($N=3$, $^*P<0.05$, $^{**}P<0.01$). Values are the mean ± SEM. **(D)** Representative western blotting images of adipogenic regulators (PPARγ, C/EBPα, and SREBP1c) and kinase module subunits (MED12, MED13, CDK8, and CCNC) at days 0, 7, 14, and 21 of adipogenesis. hASC, human adipose-derived stem cells; qRT-PCR, quantitative reverse transcriptase-PCR; SEM, standard error of the mean.

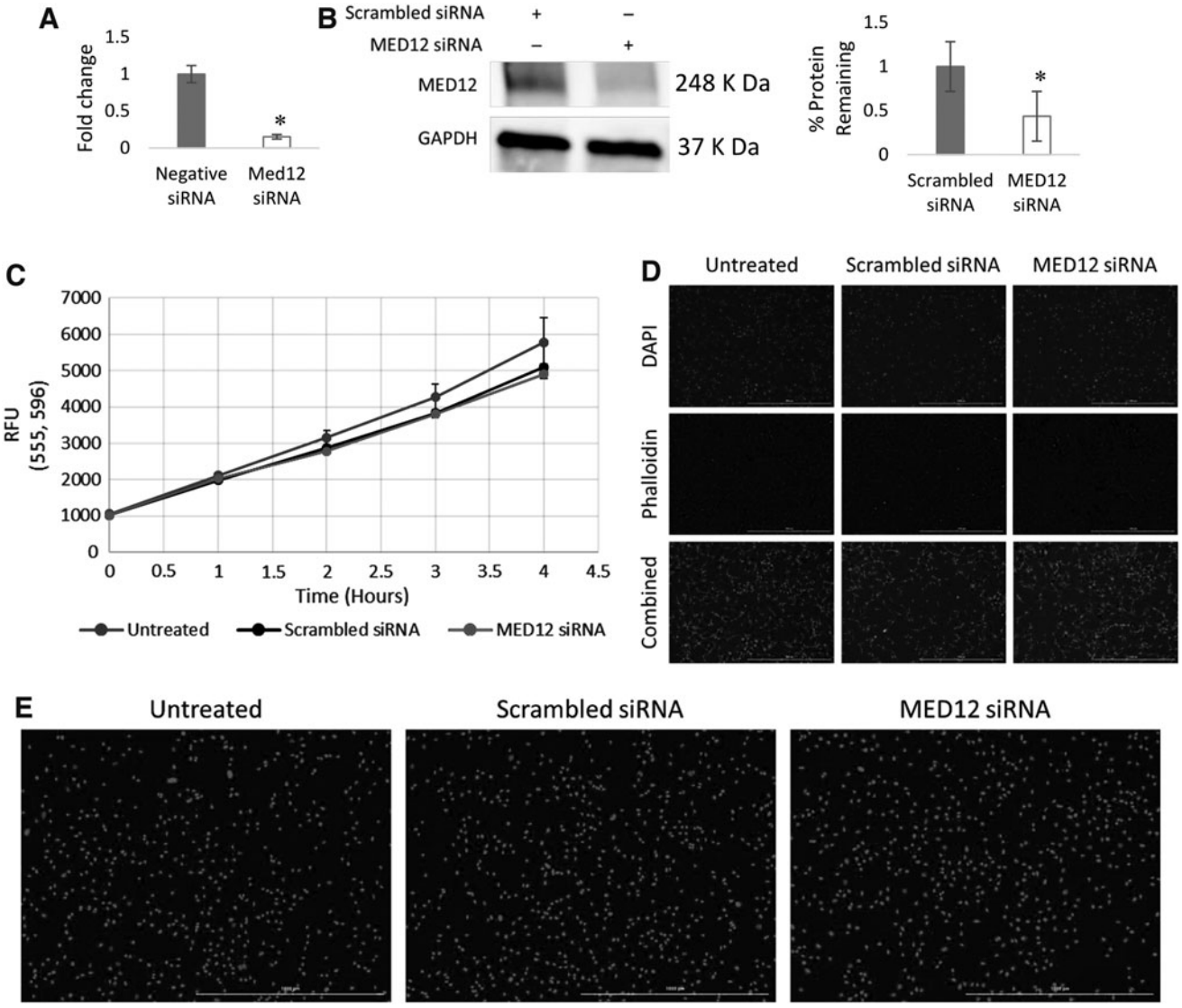

FIG. 2. Knockdown of MED12 does not affect hASC self-renewal. **(A)** Evaluation of *med12* transcript after the knockdown of MED12 in hASCs using qRT-PCR in hASCs ($N = 3$, $^*P < 0.05$). Values are the mean ± SEM. **(B)** Evaluation of MED12 protein after the knockdown of MED12 in hASCs. The graph indicates the protein level quantification using ImageJ, and the relative abundance of each band was normalized to GAPDH. **(C)** AlamarBlue assay performed 72 h after initiation of an MED12 knockdown. **(D, E)** Live/dead staining and DAPI/Phalloidin staining of cultured hASCs after 72 h after the initiation of a MED12 knockdown, respectively.

FIG. 3. Knockdown of MED12 affects adipogenesis of hASCs. **(A)** Evaluation of *med12* transcript during adipogenesis after the knockdown of MED12 in hASCs at days 3, 7, and 14 of adipogenesis using qRT-PCR ($N = 3$, $^*P < 0.05$). Values are the mean ± SEM. **(B)** Evaluation of MED12 protein after the knockdown of MED12 during adipogenesis after the knockdown of MED12 at days 3, 7, and 14 of adipogenesis in hASCs using western blot. The graph indicates the protein level quantification using ImageJ and the relative abundance of each band was normalized to GAPDH. **(C)** Phase contrast microscopy and Oil Red O staining color images of adipogenic differentiation of hASCs at days 3, 7, and 14. Stained lipid droplets are shown with *arrows*. **(D)** Evaluation of adipogenic marker *pparγ* transcript during adipogenesis after the knockdown of MED12 in hASCs at days 3, 7, and 14 using qRT-PCR. ($N = 3$, $^*P < 0.05$). Values are the mean ± SEM. **(E)** Evaluation of PPARγ protein expression at days 3, 7, and 14 of adipogenesis after the knockdown of MED12 in hASCs using western blot. The graph indicates the protein level quantification using ImageJ and the relative abundance of each band was normalized to GAPDH. **(F)** Evaluation of *med13*, *ccnc*, and *cdk8* transcript, respectively, during adipogenesis after the knockdown of MED12 knockdown at days 3, 7, and 14 ($N = 3$, $^*P < 0.05$). Values are the mean ± SEM. **(G)** Evaluation of MED13, CDK8, and CCNC protein expression at days 3, 7, and 14 of adipogenesis after MED12 knockdown using western blot.

21 days after the induction of adipogenesis. The expression of *med13* increased consistently from days 0 to 21, whereas the expression of *cdk8* dropped at day 7 then increased at days 14 and 21. In contrast, the protein levels of MED12, CDK8, and CCNC demonstrated a distinctive pattern throughout the progression of adipogenesis, where expression decreases during the middle stage and increases again during the late stage of adipogenesis, whereas MED13 expression steadily increased throughout the 21-day period (Fig. 1D).

MED12 knockdown does not affect hASC survival and proliferation

Given the increased expression of MED12 as compared with the other subunits, we next sought to determine the role of MED12 in adipogenesis. Initially, hASCs were transfected and incubated with MED12-specific siRNA for 72 h under self-renewing conditions to assess the influence of the knockdown on cell proliferation and viability. Knockdown

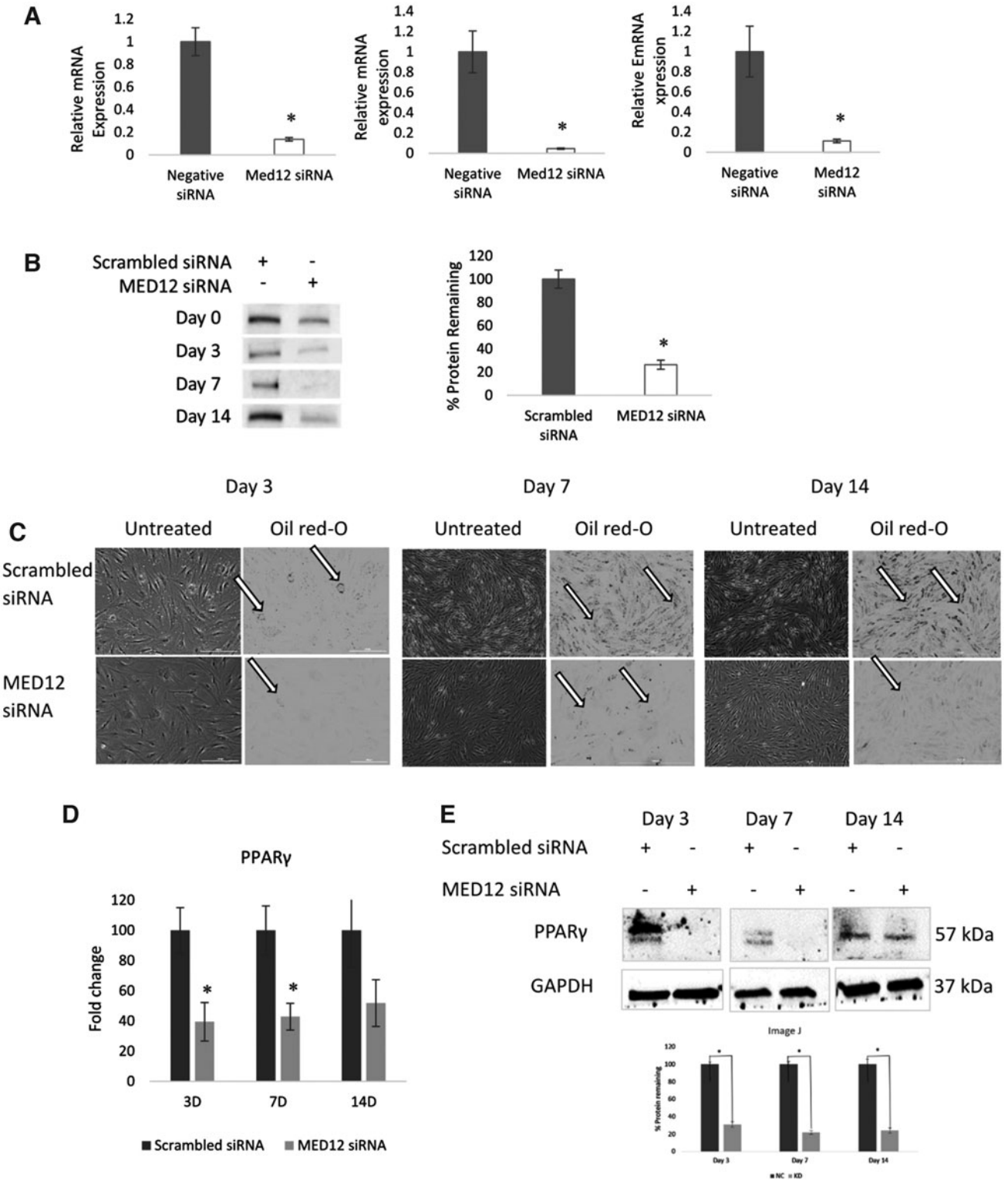

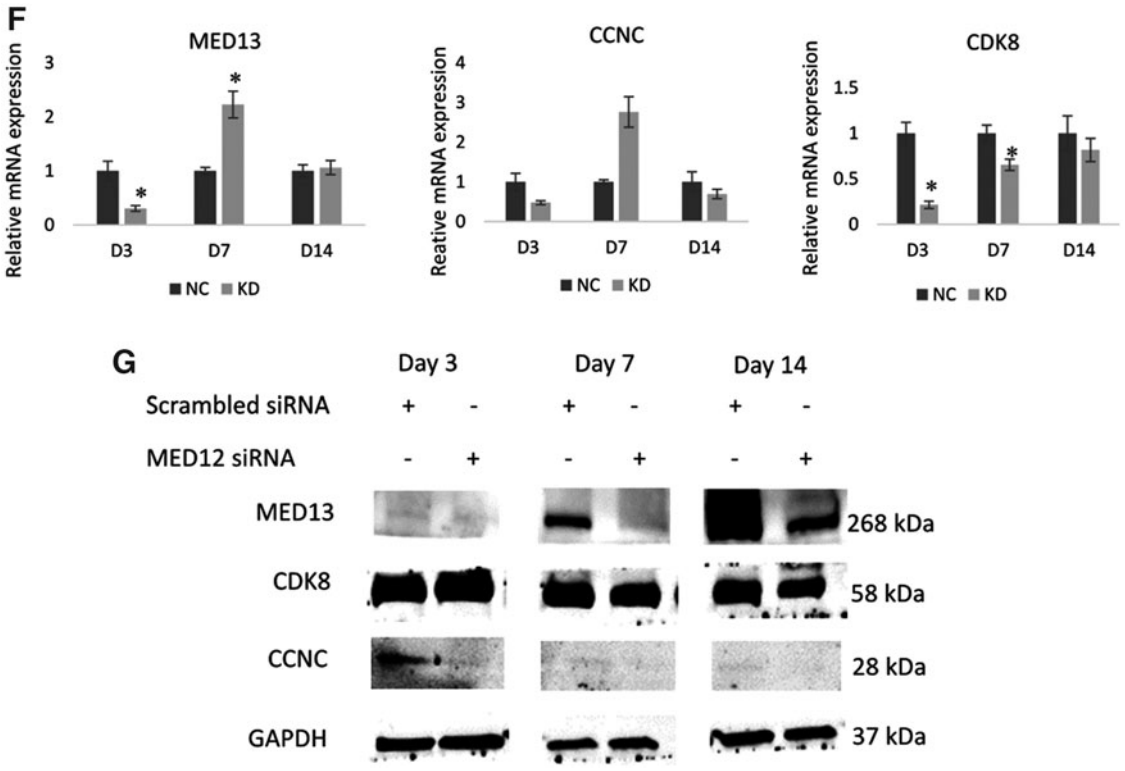

FIG. 3. (Continued).

was validated by examining transcript and protein (Fig. 2A, B) and metabolic activity and proliferation were monitored using alamarBlue assays and cell staining, respectively.

The alamarBlue assay showed a slight decrease in the rate of proliferation of hASCs after the knockdown of Med12 but no significant difference between negative control and MED12 siRNA-treated cells (Fig. 2C). A live/dead assay and a study of morphology using DAPI/Phalloidin staining, both demonstrated no significant difference between negative control and MED12 knockdown cells (Fig. 2D, E).

Knockdown of MED12 leads to decreased adipogenesis of hASCs

Given the knockdown efficiency and the minimal impact of the MED12 knockdown on hASC viability and proliferation, we aimed to characterize hASCs undergoing adipogenesis after a MED12 knockdown. Cells were transfected with MED12-specific siRNA 24 h before inducing adipogenic differentiation. Knockdown was validated using qRT-PCR (Fig. 3A) and western blog (Fig. 3B). Adipogenesis was assessed based on morphology, Oil Red O staining, and transcription factor profiles. Oil Red O staining indicated less lipid vesicle formation after the decreased expression of MED12, which was further confirmed by stain extraction and quantification (Fig. 3C).

To uncover additional molecular signatures related to adipogenesis, we examined the expression of PPARγ, a master regulator of adipogenesis. We observed that both mRNA and protein levels of PPARγ decreased with the decreased expression of MED12 (Fig. 3D, E), confirming the decrease in adipogenesis.

Knockdown of MED12 impacts expression of other kinase subunits

To determine whether knockdown of MED12 impacts the expression of other kinase module subunits, we examined both transcript and protein levels of MED13, CDK8, and CCNC after the knockdown of MED12. Given the central location of MED12 between MED13 andCDK8/CCNC in the kinase module, the decreased expression of CDK8/CCNC was expected in a MED12 knockdown.

FIG. 4. MED12 knockdown affects early adipogenesis. **(A)** Pictorial representation of the procedure of MED12 knockdown showing knockdown at different stages of adipogenesis (PD: predifferentiation, 3D: 3 days after differentiation, and 7D: 7 days after differentiation). **(B, C)** qRT-PCR and western blot to validate transcript and protein levels, respectively, of MED12 knockdown in groups PD, 3D, and 7D. **(D)** Phase contrast microscopy and Oil Red O staining color images of groups PD, 3D, and 7D. Stained lipid droplets are shown with *arrows*. Graph indicates the quantification of the stained lipid droplets performed using eluted Oil Red O stain through measuring absorbance at 510 nm. The readings were normalized to background values of noninduced control hASCs ($N=3$, $^*P<0.05$). **(E, F)** qRT-PCR and western blot analysis of transcript and protein expression of PPARγ in groups PD, 3D, and 7D, respectively. Each value represents mean ± SEM of three replicates ($N=3$, $^*P<0.05$).

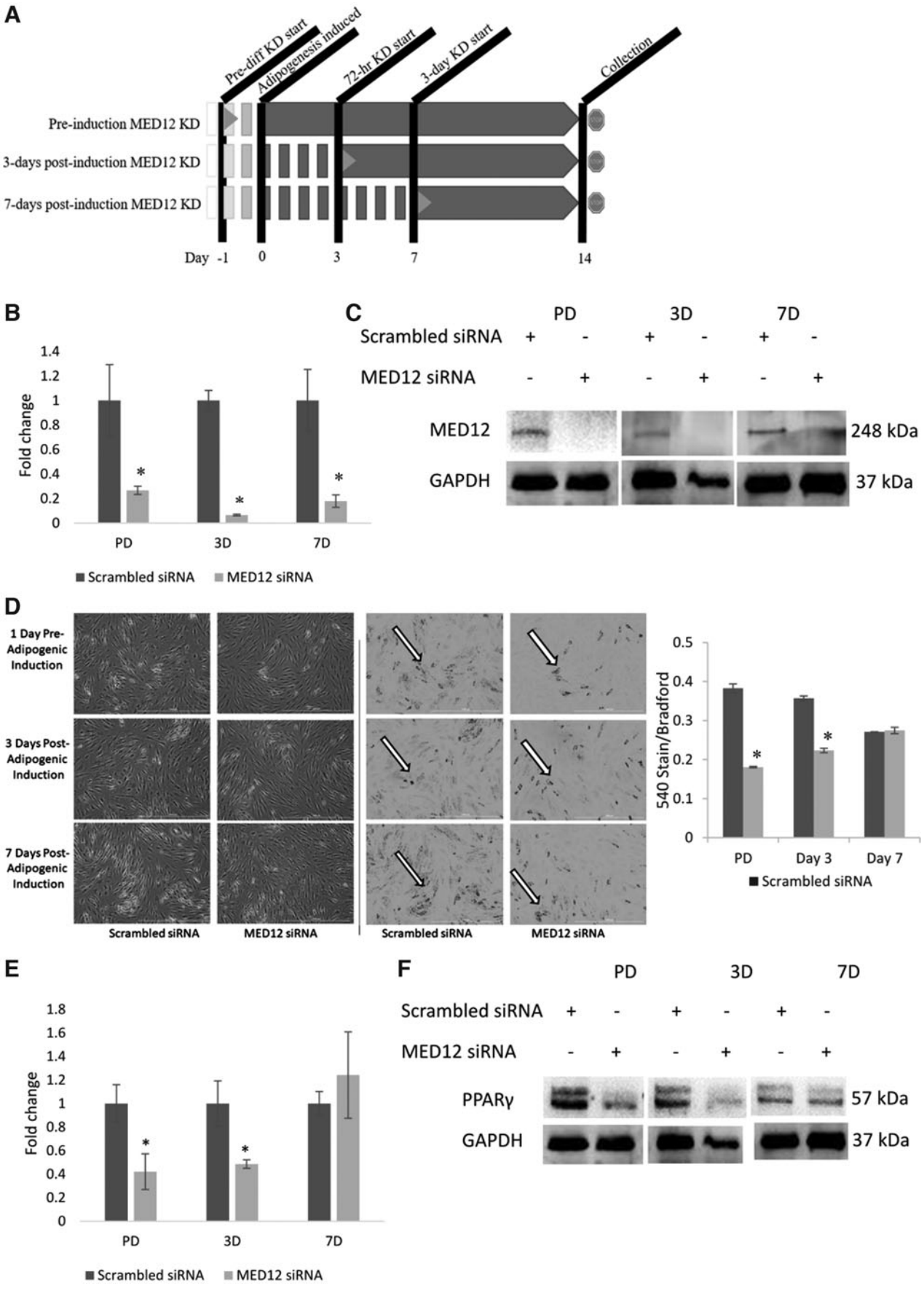
A
Pre-diff KD start
Adipogenesis induced
72-hr KD start
3-day KD start
Collection
Pre-induction MED12 KD
3-days post-induction MED12 KD
7-days post-induction MED12 KD
Day -1
0
3
7
14
B
Fold change
1.4
1.2
1
0.8
0.6
0.4
0.2
0
PD
3D
7D
Scrambled siRNA
MED12 siRNA
C
PD
3D
7D
Scrambled siRNA + - + - + -
MED12 siRNA - + - + - +
MED12
248 kDa
GAPDH
37 kDa
D
1 Day Pre-Adipogenic Induction
3 Days Post-Adipogenic Induction
7 Days Post-Adipogenic Induction
Scrambled siRNA
MED12 siRNA
Scrambled siRNA
MED12 siRNA
540 Stain/Bradford
0.5
0.4
0.3
0.2
0.1
0
PD
Day 3
Day 7
Scrambled siRNA
E
Fold change
1.8
1.6
1.4
1.2
1
0.8
0.6
0.4
0.2
0
PD
3D
7D
Scrambled siRNA
MED12 siRNA
F
PD
3D
7D
Scrambled siRNA + - + - + -
MED12 siRNA - + - + - +
PPARγ
57 kDa
GAPDH
37 kDa

Interestingly, qRT-PCR analysis of the MED12 knockdown revealed a significant change in *med13*, *cdk8*, and *ccnc* mRNA levels at days 3 and 7 of adipogenesis, whereas no significant change was observed at day 14 of adipogenesis (Fig. 3F). When protein levels were examined, the expression of CDK8 remained unchanged, whereas MED13 and CCNC demonstrated lower expression in MED12 knockdown cells compared with negative control cells throughout adipogenic differentiation (Fig. 3G).

MED12 is important during early adipogenesis

After observing the influence of MED12 on adipogenesis, we examined the contribution of MED12 during distinct stages of adipogenesis. Cells were transfected with MED12 siRNA 1-day predifferentiation (PD) as a control. Additional samples were transfected 3 days after inducing differentiation (3D), and 7 days after inducing differentiation (7D). Cells were then collected 14 days after initiating adipogenic differentiation (Fig. 4A). qRT-PCR and western blot were performed to validate MED12 knockdown at all time points (Fig. 4B, C).

Oil Red O staining and stain extraction were performed to characterize the progression of adipogenesis (Fig. 4D). Oil Red O staining demonstrated less lipid vesicle formation PD and 3D, whereas cells with MED12 siRNA 7D showed no significant change in lipid vesicle staining.

Similarly, we observed a reduction in expression of *PPARγ* with MED12 knockdowns performed PD and 3D, but no significant difference of expression in cells transfected with MED12 siRNA 7 days after inducing adipogenesis (Fig. 4E). Protein levels of PPARγ followed similar trends of reduction in cells transfected with MED12 siRNA PD or 3 days after inducing adipogenesis, but no significant difference upon MED12 knockdown 7D(Fig. 4F). This interesting shift in PPARγ expression upon MED12 knockdown 7D, along with staining data, indicates a role for MED12 during the early stages of adipogenesis.

MED12 interacts with adipogenic regulators during adipogenesis

Given the relationship observed between MED12 knockdown and PPARγ expression, we sought to examine the interaction between MED12 and PPARγ along with other adipogenic regulators including C/EBPα and SREBP1c. We performed Co-IPs during the early, middle, and late stages of adipogenesis using hASCs. As expected, the MED12 pulldown assay revealed the presence of PPARγ and C/EBPα at all time points of adipogenesis (Fig. 5A–C). Interestingly, MED12 interacts with SREBP1c only in the late stage (Fig. 5D). These results demonstrate the interaction of MED12 with transcriptional regulators of adipogenesis and support the notion that MED12 may play a role in initiating adipogenesis as well as maintaining mature adipocytes in vitro.

Co-IP experiments after MED12 knockdown showed reduced PPARγ levels in eluted samples, supporting the reduction in PPARγ after the decreased expression of MED12 (Fig. 3E). In addition, no significant reduction in

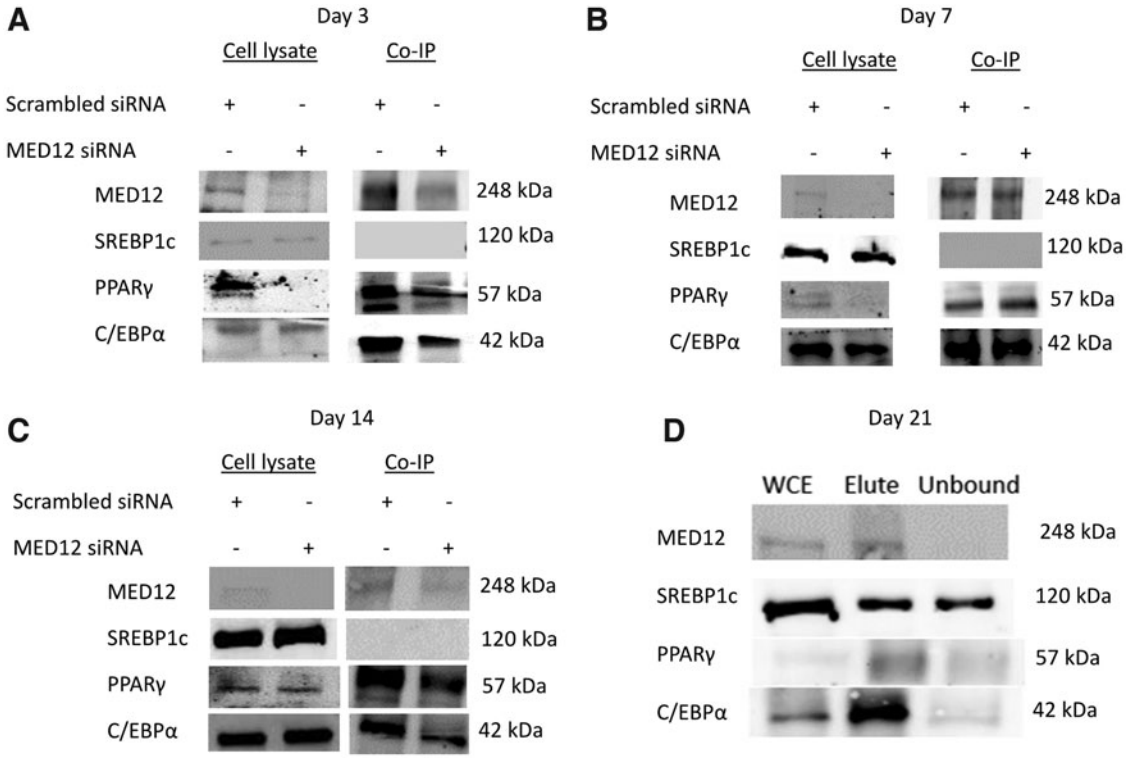

FIG. 5. MED12 interacts with adipogenic regulators during adipogenesis of hASCs. **(A–D)** Co-IP of MED12 during different stages of adipogenesis, days 3, 7, 14, and 21, respectively. Cell lysates are whole cell extracts of respective time points with negative control and MED12 knockdown. Co-IP represents the elution sample obtained after MED12 Co-IP and the unbound represents the remaining sample content that the target protein does not interact with. Co-IP, coimmunoprecipitation assay.

expression of C/EBPα was observed with the MED12 knockdown even though the interaction between these proteins is constantly present during all stages of adipogenesis. This suggests that MED12 might be regulating adipogenesis through an interaction with PPARγ.

Differential interaction of MED12 and CDK8 with adipogenic transcription factors in mouse preadipocytes and mature adipocytes

The 3T3-L1 cell line is a widely used in vitro model to study the process by which preadipocytes are differentiated into mature adipocytes. Therefore, we sought to explore the potential role of the mediator kinase subunits in these murine adipocytes. The expression of the kinase module subunits MED12, MED13, CDK8, and CCNC fluctuated throughout 7 days of adipogenic differentiation (Fig. 6A) supporting the observed expression profiles of kinase module subunits during adipogenesis of hASCs (Fig. 1C).

To further explore the interactions of kinase module subunits with adipogenic regulators, we performed IP analysis of MED12 and CDK8. Immunoblotting results showed that MED12 interacts with PPARγ, C/EBPα, and SREBP1C as well as STAT5A in both preadipocytes and mature

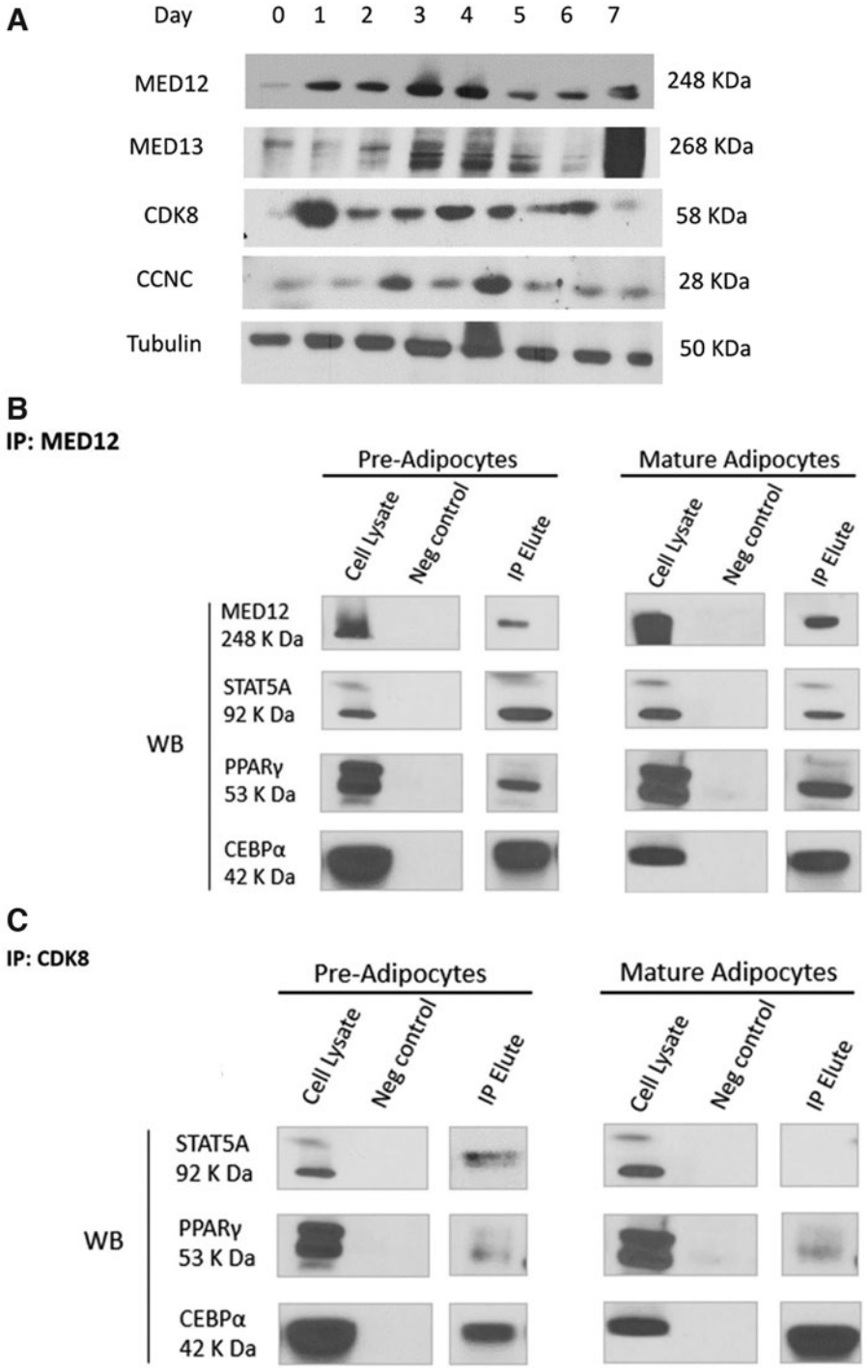

FIG. 6. Expression and interaction of kinase subunits during adipogenesis in mouse 3T3L1 cells. **(A)** Western blot to evaluate protein expression of kinase module subunits MED12, MED13, CDK8, and CCNC in cultured mouse preadipocytes differentiated into adipocytes collected at days 1 through 7. **(B, C)** Immunoprecipitation analysis of MED12 and CDK8 in mouse preadipocytes and mature adipocytes, respectively. Two hundred microliters of protein lysate collected from cultured 3T3L1 mouse preadipocytes and mature adipocytes was incubated with 5 μL of MED12 and CDK8 polyclonal antibody, respectively, and the precipitated immunocomplexes were subjected to western blot. Whole cell lysate and IP buffer were used as positive and negative control, respectively. IP elute represents the presence of respective protein present with the immunoprecipitation. Decreased expression of kinase module subunits upon feeding after fasting in specific mouse adipose tissue depots. Fourteen-week-old female mice were subjected to the fasting and feeding protocol, and adipose tissue depot extractions were performed as described in Materials and Methods section ($n = 3$ per group). **(D, E)** Representative western blot analysis of the mediator kinase module subunits from fasted and fed adipose tissue depots iWAT, gWAT, rWAT, mWAT, and BAT, respectively. BAT, brown adipose tissue; WAT, white adipose tissue.

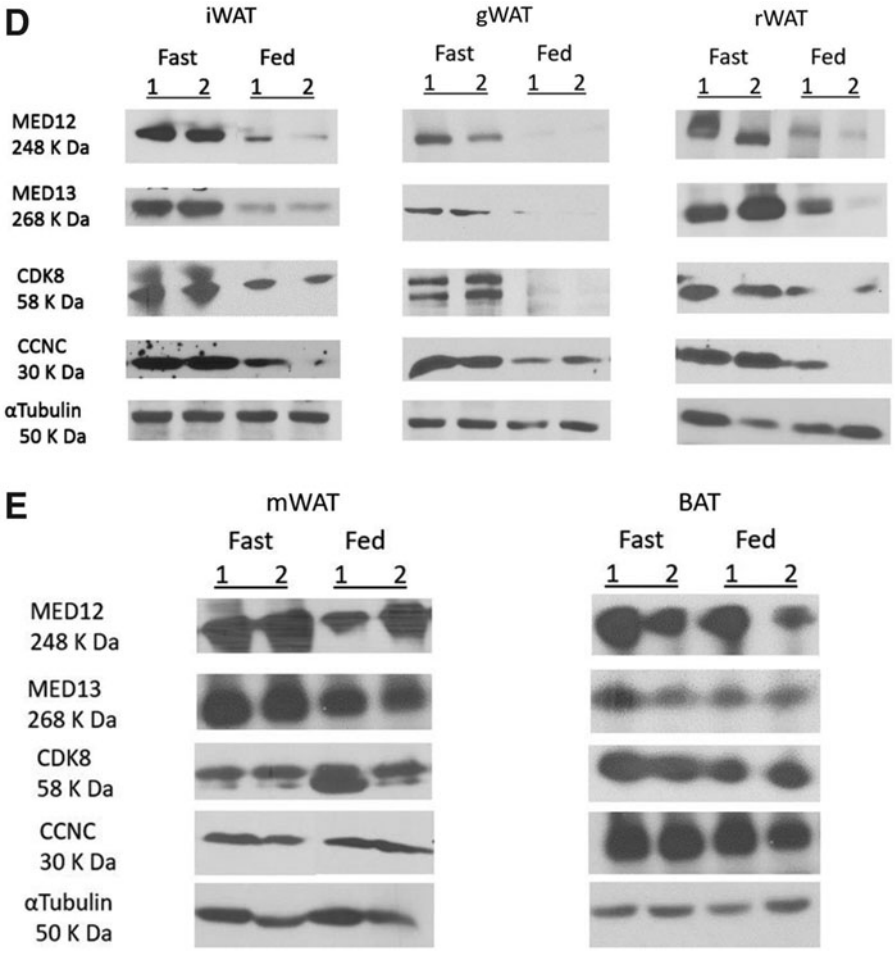

FIG. 6. (Continued).

adipocytes (Fig. 6B), whereas CDK8 interacts with C/EBPα in both preadipocytes and mature adipocytes but does not appear to interact with PPARγ and STAT5A (Fig. 6C).

Reduced expression of the kinase module subunits in iWAT, gWAT, and rWAT

Previous studies have shown that the kinase module is dissociated from the mediator complex and degraded following nutrient signals in mouse liver [30]. To determine whether the kinase module subunits of the mediator complex are also regulated by nutrient availability in other tissues, we used animal models to isolate and compare the protein levels of different fat tissue depots (iWAT, gWAT, rWAT, mWAT, and BAT) between mice that were fasted overnight and those that were fed for 4 h after the overnight fast.

As observed in previous studies, the mouse liver extracts displayed reduced levels of the kinase module subunits in the fed state. Similarly, we observed a reduction in MED12, MED13, CDK8, and CCNC in mouse adipose tissues iWAT, rWAT, and gWAT (Fig. 6D), whereas there was no significant change in expression of the kinase subunits in tissues mWAT and BAT (Fig. 6E).

Discussion

The mediator complex links a vast majority of regulated transcription factors with the basal transcription machinery, playing a critical role in cell type-specific gene expression. Despite evidence for the role of MED12 in early development and cell fate determination and its requirement in structural integrity and function of the mediator complex [20–22], within the context of metabolism, MED12 remains a poorly characterized subunit. Here, we provide evidence suggesting that the mediator kinase subunit MED12 is a critical regulator of adipogenesis. Knockdown of MED12 in hASCs decreased adipogenic progression, indicating a specific role in adipogenesis.

It is noteworthy that another mediator kinase subunit, CCNC, is also identified as a novel regulator of adipogenesis by activating C/EBPα-dependent transcription in 3T3-L1 cells [31]. As MED12 knockdown in hASCs prevented induction of PPARγ, we can speculate that MED12 regulates adipogenesis through PPARγ. However, unlike CCNC, MED12 plays a role in facilitating PPARγ expression, since MED12 knockdown had no effect on expression of C/EBPα (Fig. 5A).

To understand the stage-specific role of MED12 in hASCs, we knocked down MED12 at early and late stages of adipogenic differentiation. Interestingly, the knockdown did not significantly decrease differentiation during late stages of adipogenesis. This inability of the MED12 knockdown to block adipocyte differentiation supports the possibility that MED12 is required during early stages of adipogenic differentiation and is supported by the overall decreased expression of MED12 during late stage of hASC adipogenesis (Fig. 1E).

Other mediator subunits have been reported to play key roles in adipogenesis during very early and late stages of adipogenesis [17,32,33]. Therefore, it is likely that the mediator complex, through different subunits, is recruited to key transcription factors at different stages of adipogenesis and thus regulates adipogenesis at different stages.

In mice, fasting followed by feeding resulted in reduced expression of the kinase module subunits in certain adipose tissue depots (iWAT, gWAT, and rWAT). However, expression of kinase module subunits remains unchanged in mWAT and BAT. Although the regulation and mechanism of the dissociation and degradation of the kinase module subunits remain unclear, these data, along with what is described in recent literature, suggest that the previous identification of size oscillation of the mediator complex through mTORC1 activation with nutrient signaling in mouse livers [30] might be replicated in certain adipose tissues.

Previous research provides evidence that in vivo hepatic mTORC1 activation leads to the activation of lipogenic gene expression [29,30]. However, it is yet to be determined whether mTORC1 activation is necessary for activation of gene expression during lipogenesis in adipose tissue. Overall, this study, along with growing evidence from other studies, suggests that mediator kinase subunits function as a control center in directing diverse metabolic processes that may provide novel strategies to target obesity and its associated diseases.

Conclusions

The mediator complex is an indispensable part of cell type-specific gene regulation in hASCs. The kinase module plays a prominent role in gene expression, and our results point to MED12 involvement beyond cell fate determination and into the maintenance of differentiated adipocytes. Of note, our data, showing sufficient evidence linking MED12 and PPARγ and other adipogenic regulators through protein–protein interactions, have illuminated the possibility that these critical regulators act in concert during adipogenesis even into the later stages of differentiation.

In addition, the regulation of kinase subunit expression in some WAT depots with nutrient availability indicates a possible regulation of associated metabolic pathways. Taken together, this study suggests the possibility of MED12 promoting and maintaining adipogenesis in vitro and the kinase module as an important contributor to downstream metabolic responses.

Acknowledgments

The authors thank Claire Peterson and Jamie Sparkman for optimizing primers and Dr. Allison Richard, Hardy Hang, and Dr. Jasmine Burrell for their expertise and guidance.

Author Disclosure Statement

No competing financial interests exist.

Funding Information

Research reported in this publication was supported by an institutional development award (IDeA) from the National Institute of General Medical Sciences of the National Institutes of Health under Grant No. P2O GMI03424-20.

References

1. Grundy SM. (2000). Metabolic complications of obesity. Endocrine 13:155–165.
2. Garrow JS. (1988). *Obesity and Related Diseases*. Churchill Livingstone, Edinburgh.
3. Flegal KM, MD Carroll, RJ Kuczmarski and CL Johnson. (1998). Overweight and obesity in the United States: prevalence and trends, 1960–1994. Int J Obes 22:39–47.
4. Guglielmi V and P Sbraccia. (2018). Obesity phenotypes: depot-differences in adipose tissue and their clinical implications. Eat Weight Disord 23:3–14.
5. Chait A and LJ Den Hartigh. (2020). Adipose tissue distribution, inflammation and its metabolic consequences, including diabetes and cardiovascular disease. Front Cardiovasc Med 7:22.
6. Palou M, T Priego, J Sánchez, AM Rodríguez, A Palou and C Picó. (2009). Gene expression patterns in visceral and subcutaneous adipose depots in rats are linked to their morphologic features. Cell Physiol Biochem 24:547–556.
7. Schoettl T, IP Fischer and S Ussar. (2018). Heterogeneity of adipose tissue in development and metabolic function. J Exp Biol 221:jeb162958
8. Sanchez-Gurmaches J, CM Hung and DA Guertin. (2016). Emerging complexities in adipocyte origins and identity. Trends Cell Biol 26:313–326.
9. Cheng L, J Wang, H Dai, Y Duan, Y An, L Shi, Y Lv, H Li, C Wang, et al. (2021). Brown and beige adipose tissue: a novel therapeutic strategy for obesity and type 2 diabetes mellitus. Adipocyte 10:48–65.
10. Al-Sulaiti H, SA Dömling and MA Elrayess. (2019). *Mediators of Impaired Adipogenesis in Obesity-Associated Insulin Resistance and T2DM in Adipose Tissue—An Update*. Intechopen. [Epub ahead of print]; DOI: 10.5772/intechopen.88746.
11. Zhang K, X Yang, Q Zhao, Z Li, F Fu, H Zhang, M Zheng and S Zhang. (2020). Molecular Mechanism of Stem Cell Differentiation into Adipocytes and Adipocyte Differentiation of Malignant Tumor. Stem Cells Int 2020:8892300.
12. Gregoire FM, CM Smas and HS Sul. (1998). Understanding adipocyte differentiation. Physiol Rev 78:783–809.
13. Farmer SR. (2005). Regulation of PPARγ activity during adipogenesis. Int J Obes 29:S13–S16.
14. Linhart HG, K Ishimura-Oka, F Demayo, T Kibe, D Repka, B Poindexter, RJ Bick and GJ Darlington. (2001). C/EBPα is required for differentiation of white but not brown adipose tissue. Proc Natl Acad Sci U S A 98:12532–12537.
15. Sarjeant K and JM Stephens. (2012). Adipogenesis. Cold Spring Harb Perspect Biol 4. https://cshperspectives.cshlp.org/content/4/9.toc.
16. Rosen ED and BM Spiegelman. (2000). Molecular regulation of adipogenesis. Annu Rev Cell Dev Biol 16:145–171.
17. Bai L, Y Jia, N Viswakarma, J Huang, A Vluggens, NE Wolins, N Jafari, MS Rao, J Borensztajn, G Yang and JK Reddy. (2011). Transcription coactivator mediator subunit MED1 Is required for the development of fatty liver in the mouse. Hepatology 53:1164–1174.
18. Allen BL and DJ Taatjes. (2015). The Mediator complex: a central integrator of transcription. Nat Rev Mol Cell Biol 16:155–166.
19. Verger A, D Monté and V Villeret. (2019). Twenty years of Mediator complex structural studies. Biochem Soc Trans 47:399–410.

20. Clark AD, M Oldenbroek and TG Boyer. (2015). Mediator kinase module and human tumorigenesis. Crit Rev Biochem Mol Biol 50:393–426.
21. Straub J, S Venigalla and JJ Newman. (2020). Mediator's Kinase Module: a modular regulator of cell fate. Stem Cells Dev 29:1535–1551.
22. Zhang S, R O'Regan and W Xu. (2020). The emerging role of mediator complex subunit 12 in tumorigenesis and response to chemotherapeutics. Cancer 126:939–948.
23. Klatt F, A Leitner, IV Kim, H Ho-Xuan, EV Schneider, F Langhammer, R Weinmann, MR Müller, R Huber, G Meister and CD Kuhn. (2020). A precisely positioned MED12 activation helix stimulates CDK8 kinase activity. Proc Natl Acad Sci U S A 117:2894–2905.
24. Keightley M-C, JE Layton, JW Hayman, JK Heath and GJ Lieschke. (2011). Mediator subunit 12 is required for neutrophil development in zebrafish. PLoS One 6:e23845.
25. Tutter AV, MP Kowalski, GA Baltus, V Iourgenko, M Labow, E Li and S Kadam. (2009). Role for Med12 in regulation of Nanog and Nanog target genes. J Biol Chem 284:3709–3718.
26. Vogl MR, S Reiprich, M Kuspert, T Kosian, H Schrewe, K-A Nave and M Wegner. (2013). Sox10 cooperates with the mediator subunit 12 during terminal differentiation of myelinating glia. J Neurosci 33:6679–6690.
27. Aranda-Orgilles B, R Saldaña-Meyer, E Wang, E Trompouki, A Fassl, S Lau, J Mullenders, PP Rocha, R Raviram, et al. (2016). MED12 regulates HSC-specific enhancers independently of mediator kinase activity to control hematopoiesis. Cell Stem Cell 19:784–799.
28. Papadopoulou T, A Kaymak, S Sayols and H Richly. (2016). Dual role of Med12 in PRC1-dependent gene repression and ncRNA-mediated transcriptional activation. Cell Cycle 15:1479–1493.
29. Feng D, DY Youn, X Zhao, Y Gao, WJ Quinn, AM Xiaoli, Y Sun, MJ Birnbaum, JE Pessin and F Yang. (2015). mTORC1 down-regulates cyclin-dependent kinase 8 (CDK8) and cyclin C (CycC). PLoS One 10.
30. Yeon Youn D, AM Xiaoli, H Kwon, F Yang and JE Pessin. (2019). The subunit assembly state of the Mediator complex is nutrient-regulated and is dysregulated in a genetic model of insulin resistance and obesity. J Biol Chem 119: 007850.
31. Song Z, AM Xiaoli, Q Zhang, Y Zhang, EST Yang, S Wang, R Chang, ZD Zhang, G Yang, et al. (2017). Cyclin C regulates adipogenesis by stimulating transcriptional activity of CCAAT/enhancer-binding protein α. J Biol Chem 292:8918–8932.
32. Zhang Y, Xiaoli, X Zhao and F Yang. (2013). The mediator complex and lipid metabolism. J Biochem Pharmacol Res 1:51–55.
33. Youn DY, AM Xiaoli, JE Pessin and F Yang. (2016). Regulation of metabolism by the Mediator complex. Biophys Rep 2:69–77.

Address correspondence to:
Dr. Jamie J. Newman
School of Biological Sciences
Louisiana Tech University
Ruston, LA 71272
USA

E-mail: jjnewman@latech.edu

Received for publication November 16, 2021
Accepted after revision December 30, 2021
Prepublished on Liebert Instant Online January 12, 2022